PROCEEDINGS B

royalsocietypublishing.org/journal/rspb

Research

Cite this article: Lapsansky AB, Kreyenmeier P, Spering M, Wylie DR, Altshuler DL. 2025 Hummingbirds use compensatory eye movements to stabilize both rotational and translational visual motion. *Proc. R. Soc. B* **292**: 20242015.
https://doi.org/10.1098/rspb.2024.2015

Received: 22 August 2024
Accepted: 15 November 2024

Subject Category:
Neuroscience and cognition

Subject Areas:
neuroscience, biomechanics

Keywords:
optokinetic response (OKR), hummingbird, oculomotor behavior, eye movement, vision

Authors for correspondence:
Anthony B. Lapsansky
e-mail: tony.lapsansky@gmail.com
Douglas L. Altshuler
e-mail: doug.altshuler@ubc.ca

Electronic supplementary material is available online at.

THE ROYAL SOCIETY PUBLISHING

Hummingbirds use compensatory eye movements to stabilize both rotational and translational visual motion

Anthony B. Lapsansky[1,2], Philipp Kreyenmeier[3], Miriam Spering[3,4], Douglas R. Wylie[5] and Douglas L. Altshuler[2,4]

[1]Salish Sea Research Center, Northwest Indian College, Bellingham, WA 98226, USA
[2]Department of Zoology, University of British Columbia, Vancouver, British Columbia V6T 1Z4, Canada
[3]Department of Ophthalmology & Visual Sciences, University of British Columbia, Vancouver, British Columbia V5Z 3N9, Canada
[4]Djavad Mowafaghian Centre for Brain Health, University of British Columbia, Vancouver, British Columbia V6T 1Z3, Canada
[5]Department of Biological Sciences, University of Alberta, Edmonton, Alberta T6G 2R3, Canada

ABL, 0000-0001-7530-7830; DLA, 0000-0002-1364-3617

To maintain stable vision, behaving animals make compensatory eye movements in response to image slip, a reflex known as the optokinetic response (OKR). Although OKR has been studied in several avian species, eye movements during flight are expected to be minimal. This is because vertebrates with laterally placed eyes typically show weak OKR to nasal-to-temporal motion (NT), which simulates typical forward locomotion, compared with temporal-to-nasal motion (TN), which simulates atypical backward locomotion. This OKR asymmetry is also reflected in the pretectum, wherein neurons sensitive to global visual motion also exhibit a TN bias. Hummingbirds, however, stabilize visual motion in all directions through whole-body movements and are unique among vertebrates in that they lack a pretectal bias. We therefore predicted that OKR in hummingbirds would be symmetrical. We measured OKR in restrained hummingbirds by presenting gratings drifting across a range of speeds. OKR in hummingbirds was asymmetrical, although the direction of asymmetry varied with stimulus speed. Hummingbirds moved their eyes largely independently of one another. Consistent with weak eye-to-eye coupling, hummingbirds also exhibited disjunctive OKR to visual motion simulating forward and backward translation. This unexpected oculomotor behaviour, previously unexplored in birds, suggests a potential role for compensatory eye movements during flight.

1. Introduction

Animals stabilize their gaze and body position in response to visual motion. In vertebrates, stabilization is achieved through two visually driven reflexes: the optokinetic response (OKR) and the optomotor response (OMR) [1]. These reflexes are highly conserved [2] and compensate for image slip across the retina through rotations of the eyes and movement of the body, respectively. Together with the vestibulo-ocular reflex, OKR and OMR work to prevent visual blurring and facilitate perception of both object motion and self-motion [3,4].

Among vertebrates, hummingbirds are experts at stabilizing visual motion and are unique among birds in their ability to sustain hovering. Substantial research effort has focused on how hummingbirds control hovering flight, aiming to understand both their behavioural guidance strategy [5,6] and the neurobiology underlying hummingbird motion processing [7,8].

Previous work has shown that hummingbirds rely on visual cues to control nectar feeding [9] and exhibit a robust OMR to both translational [5,10] and rotational stimuli [11]. Additionally, perched hummingbirds respond to rotational stimuli by rotating their heads [12], a gaze-stabilizing behaviour termed the optocollic response (OCR). However, despite the clear importance of visual stabilization in these animals, it is currently unknown whether hummingbirds also stabilize visual motion through eye movements, and how OKR in hummingbirds would compare with that in other vertebrates.

In many vertebrates, especially those with lateral eyes like hummingbirds, the strength of OKR varies with the direction of motion [13,14]. For animals with an asymmetrical OKR, monocular stimuli moving in the temporal-to-nasal (TN) direction evoke OKR with higher gains (ratio between eye and stimulus speed) than those moving in the nasal-to-temporal (NT) direction. This peculiar asymmetry has been documented across diverse taxa, including in mammals, birds, non-avian reptiles, amphibians and fish (reviewed by [13]). For consistency with these and other studies of non-humans, we refer to the slow tracking response driven by visual motion as OKR, whereas we refer to the sawtooth pattern of alternating slow and quick eye movements as optokinetic nystagmus (OKN).

The asymmetry of OKR is widely viewed as an evolutionary adaptation to prevent compensatory eye movements during locomotion [15–19]. The global visual motion produced by locomotion, termed optic flow, provides a rich source of information useful for guidance [20,21]. As they move forward through the environment, lateral-eyed animals experience predominantly NT visual motion across both eyes. Therefore, by suppressing the OKR in response to NT stimuli, animals preserve optic flow for self-motion perception. The situation is more complicated for walking in birds, during which some species periodically compensate for bilateral NT motion with OCR, i.e. the head-bobbing typical of pigeons and others [22,23]. However, pigeons, and likely other species as well, switch to a strategy of minimizing head accelerations during steady flight [24,25], thereby preserving optic flow signals.

While there are only a few published studies on translational OKR, their findings are generally consistent with those of monocular OKR. Translational OKR is studied by presenting stimuli moving in parallel, simulating forward locomotion if both sides are presented stimuli drifting NT (progressive) and backward locomotion if both sides are presented stimuli drifting TN (regressive). Goldfish (*Carassius auratus*) and butterflyfish (*Chaetodon rainfordi*) exhibit convergence of the two eyes in response to regressive stimulation but do not respond to progressive stimulation [17,26]. Sandlance (*Limnichthyes fasciatus*), pipefish (*Corythoichthyes intestinalis*), larval zebrafish (*Danio rerio*) and rabbits (*Oryctolagus cuniculus*) exhibit convergence and divergence in response to regressive and progressive stimulation, respectively, although the response to progressive stimulation is relatively weak [16,26,27].

It is unknown whether hummingbirds exhibit OKR in response to rotational and translational motion and if they do, whether it follows the same asymmetric pattern as in many other lateral-eyed animals. Here, we explored OKR in Anna's hummingbirds (*Calypte anna*), an emerging model for visual guidance and optic flow processing. The null expectation is for Anna's hummingbirds to exhibit OKR like that in other birds, in which TN stimuli evoke stronger OKR than NT stimuli. However, there are several reasons to predict that OKR in hummingbirds might differ from that found in other birds.

First, unlike most other animals, hummingbirds routinely experience TN in addition to NT visual motion. During hovering, for example, hummingbirds can drift in any direction owing to wind and they frequently fly backwards as they pull away from feeders or flowers. Thus, hummingbirds may suppress compensatory eye movements in response to both NT and TN visual motions.

Second, the neural substrates of OKR in hummingbirds differ from those of other birds. Across vertebrates, optic flow is encoded by nuclei within the accessory optic system (AOS) and pretectum. These nuclei, respectively termed the nucleus of the basal optic root (nBOR) and pretectal nucleus lentiformis mesencephali (LM) in birds, receive direct input from the retina and project to the cerebellum, forming a subcortical pathway for processing optic flow [28]. The roles of the AOS and pretectum in OKR are well established and highly conserved across taxa [2,13]. In birds, ablation of the LM eliminates OKR to TN stimuli presented to the affected side, whereas ablation of nBOR eliminates OKR to NT stimuli presented to the affected side [29,30]. These complementary functions are reflected in the motion preferences of neurons within LM and nBOR. In nBOR, neurons that respond preferentially to stimuli moving upward, downward or in the NT direction are well-represented, whereas neurons that prefer TN are extremely rare [31,32]. In the LM of pigeons (*Columba livia*) and zebra finches (*Taeniopygia guttata*), a strong majority of the neurons respond best to TN motion [33–35], matching OKR asymmetry in these species [36,37]. The situation appears different in hummingbirds, however. Not only is the LM of hummingbirds massively hypertrophied compared with other birds [8], but the distribution of direction preferences in the hummingbird LM does not exhibit any overall population bias [7,33]. As the tuning of OKR is expected to match that of the corresponding neural substrate, and does for other birds, the lack of population bias in the hummingbird LM may produce symmetrical OKR.

Given hummingbirds' unique locomotor behaviour and neurophysiology, we predicted that Anna's hummingbirds would exhibit a symmetrical horizontal OKR. To test this prediction, we developed a system to record binocular oculomotor behaviour in head-restrained hummingbirds in response to drifting gratings using high-speed videography. In addition to monocular and binocular rotational treatments, we tested OKR to binocular translational stimuli, motivated by a recent study showing that hovering hummingbirds respond to translating gratings with robust and approximately symmetrical OMR [5].

2. Material and methods

(a) Animals

Six adult male Anna's hummingbirds (*C. anna*) were caught on the University of British Columbia campus (07 Feburary 2022–04 March 2023). Animals were individually housed in 0.61 m × 0.61 m × 0.91 m cages and provided with ad libitum artificial nectar (Nektar-Plus, Nekton, Pforzheim, Germany & Nectar 9, Roudybush, Woodland, CA, USA). All procedures were approved by the University of British Columbia Animal Care Committee in accordance with the guidelines set out by the Canadian Council on Animal Care. Animals were released back to the wild following the experiments described herein.

(b) Method of restraint

To allow the release of the birds after our experiments, we developed a method for non-invasive restraint of hummingbirds. Head-restraint is required to study OKR in the absence of the vestibulo-ocular reflex. We restrained hummingbirds in a flight posture by wrapping them in an elastic 'ACE Brand' bandage (3M, Maplewood, USA) and placing them on a plastic bed tilted 10° above horizontal (see figure 1*a*). To restrain the head, we fashioned a bill guide using the opening of a 30 ml Luer syringe (Henke Sass Wolf, Dudley, USA). The bill guide was oriented to hold the bill horizontally, as is typical in flight (figure 1*b*).

Birds were hand-fed a sucrose solution before each recording session. We then wrapped the bird in the elastic bandage, gently positioned the bill through the guide and placed the animal on the plastic bed. We were careful to place the body close enough to the bill guide so that the animals were unable to retract their head. Extension of the head was prevented as the opening of the bill guide was smaller than the widest part of the bill. After each recording session, animals were returned to their home cage.

(c) Eye tracking

An overview of the eye-tracking setup is provided in figure 1. We used a bright pupil method to detect and track both eyes of each hummingbird [38]. Two cameras were positioned using tripods on the left- and right-sides of the bird, at the height of the animal and along the optical axis of the eyes (approx. 20 deg nasal from lateral). Bright pupil eye tracking uses an infrared light (IR) to increase the contrast between the pupil and the iris (analogous to the 'red eye effect'). For illumination, we used 850 nm IR ring lights (Feyond FY76−72V4-F, Shenzhen City, China). These IR lights were attached to 50 mm Nikkor camera lenses (Kabushiki-gaisha Nikon, Tokyo, Japan). Videos were acquired using IR-sensitive cameras (Prosilicia GE680, Allied Vision, Stadtroda, Germany) operating at 120 Hz with recording performed using Streampix v. 6 (NorPix Inc., Montreal, Canada). Recording occurred in the dark. The IR lights produce illumination outside of the visual range for hummingbirds [39].

(d) Visual stimuli

Stimuli were generated using PsychoPy v. 2023.1.3 [40] and presented on two 144 Hz LCD monitors (ASUS VG248QG, ASUSTeK Computer Inc., Taipai, Taiwan) set to sRGB colour mode, resulting in gratings with a Michelson contrast of 0.99. The monitors were oriented perpendicular to the bird and positioned 30 cm away on either side (figure 1*a*). To allow a clear view of the bird for each camera, the monitors were height-adjusted so that the lower margin of the screen was just below that of the bird. Thus, visual stimuli were presented to the upper and lateral visual fields, occupying *ca* 83 deg horizontally and *ca* 45 deg vertically on either side of the animal.

Previous electrophysiology studies in hummingbirds used random dot fields to determine neuron direction preferences and then sinewave gratings to measure spatiotemporal tuning in the preferred direction [7,31,33]. We selected stimulus conditions to match these studies but used sinewave gratings throughout. This allowed us to assess OKR at stimulus speeds beyond what we could produce with dots and to replicate stimulus speeds across a consistent set of spatial and temporal frequencies (table 1).

Within a recording session, we randomized the direction (NT or TN) and speed of stimuli presented on each monitor. Hummingbirds must feed frequently, limiting the maximum length of recording sessions to under 40 min. We therefore presented stimuli for each spatial frequency on separate days, except for spatial frequencies of 0.015625 cyc deg^{-1} and 4 cyc deg^{-1}, which were presented on the same day but with a feeding break in between. Stimulus velocity was defined as the product of temporal and spatial frequency (table 1). During binocular stimulation, stimulus speeds presented to both eyes were always matched (e.g. 1 deg s^{-1} TN to the right eye and 1 deg s^{-1} NT to the left eye).

Each recording session consisted of a set of trials repeated three times and randomized within each set. Each trial began with a static pattern for 1 s, followed by a stationary sinewave grating for 1 s, followed by 10 s of motion of that same sinewave grating in either the TN or NT direction. As we did not wish to physically cover an eye for monocular trials and risk injury to the birds, two methods were used for monocular stimulation: (i) the monitor for the unstimulated eye was either turned grey after the static pattern (ii) or changed to the sinewave grating but held stationary. We analysed data from the former method because the latter represents an unequal speed combination, although data from both methods were qualitatively similar. For binocular trials, the stimulus direction for each monitor was set independently to produce either regressive stimulation (TN & TN), progressive stimulation (NT & NT) or rotation ((TN & NT) or (NT & TN)). We refer to binocular NT & TN combinations as rotational stimulation; however, as our stimulus monitors did not curve around the animal, these conditions technically represent pseudo-rotation.

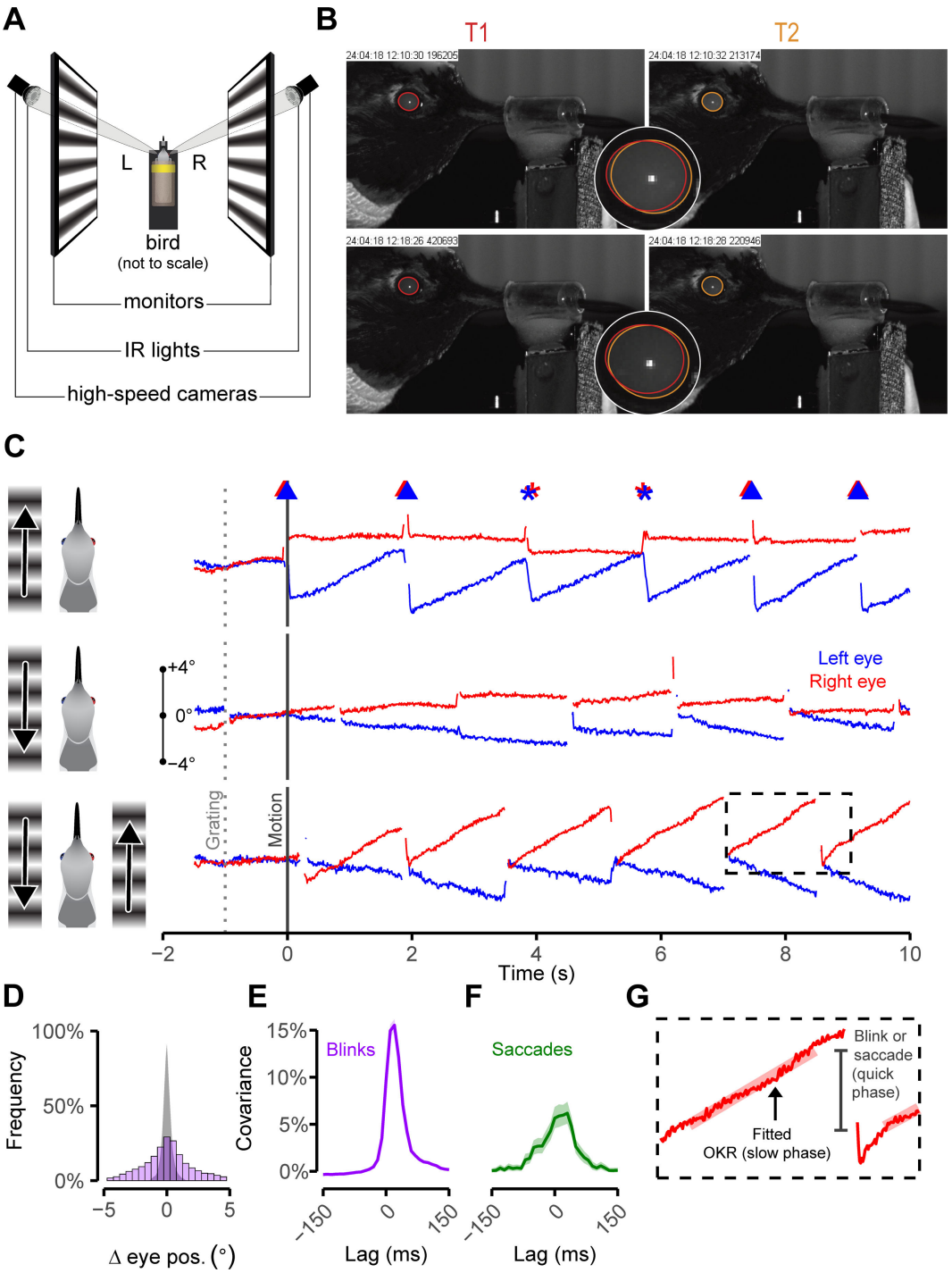

Figure 1. Hummingbirds exhibit compensatory eye movements in response to visual motion. (A) Hummingbirds were restrained with the head oriented horizontally, dorsal side up. Stimuli were presented perpendicular to the animal and on either side (L—left, R—right). High-speed cameras recorded the position of the pupil, illuminated using IR lights. (B) Two examples of eye position change between successive time points (T1 and T2). An additional example is shown in electronic supplementary material, video 1. Eye position was determined by tracking the pupil, which appeared as a light-coloured oval under IR illumination. Eye movements were small but repeatable. See electronic supplementary material, video1 for an animated alternative to this figure panel. (C) Horizonal eye position during representative trials, aligned to motion onset. Trials consisted of 1 s of visual static, followed by 1 s of a static grating and then by 10 s of motion of that same grating. Representative responses to monocular TN (top), NT (middle) and binocular rotary (bottom) stimulation. In these examples, stimuli were at 1 cyc deg^{-1} and 4 deg s^{-1}. Timing of blinks (triangles) and saccades (stars) for the upper trial are indicated above. Data for left eye in blue and right eye in red. Positive is defined as nasalward for both eyes. (D) The magnitude of changes to eye position occurring during blinks (purple) compared with the null expectation (grey), generated by repeated sampling across random time windows. Changes in eye position were significantly larger during blinks than the null expectation ($p < 0.001$; permutation test), suggesting coordination between rapid eye movements and blinking. (E, F) Timing was correlated between the eyes for both blinking (E)—detected using the position of the eyelids—and saccades (F), detected using eye velocity. See also the upper trial in (C). (G) To separate and extract OKR and rapid eye movements, we fit linear regressions to the eye position between each blink or saccade. The slope of these fits represents OKR velocity. The offset between endpoints of adjacent fits represents the magnitude and direction of rapid eye movements. Data from lower example in (C).

Table 1. Stimulus used to study OKR, arranged by spatial frequency (rows) and temporal frequency (columns). Stimulus velocity was defined as the product of spatial and temporal frequency.

	temporal frequency (Hz)				
spatial frequency (cyc deg^{-1})	**0.0625**	**0.25**	**1**	**4**	**16**
0.015625	4 deg s^{-1}	16 deg s^{-1}	64 deg s^{-1}	256 deg s^{-1}	—
0.0625	1 deg s^{-1}	4 deg s^{-1}	16 deg s^{-1}	64 deg s^{-1}	256 deg s^{-1}
0.25	0.25 deg s^{-1}	1 deg s^{-1}	4 deg s^{-1}	16 deg s^{-1}	64 deg s^{-1}
1	—	0.25 deg s^{-1}	1 deg s^{-1}	4 deg s^{-1}	16 deg s^{-1}
4	—	—	0.25 deg s^{-1}	1 deg s^{-1}	4 deg s^{-1}

(e) Analysis of oculomotor behaviour

To extract the position of the pupil from each video, we used a combination of thresholding and contour segmentation in python v. 3.11.8 [41]. We trained a custom DeepLabCut [42] model (ResNet 152) to track the corneal reflection and eyelids. To track the pupil, we used data from the same DeepLabCut model to determine a region-of-interest around the eye, upscaled this portion of the video frame and then used thresholding and contour detection in OpenCV v. 4.9.0 [43] for pupil detection.

Analysis of raw pupil position was performed in MATLAB R2023b [44]. We first removed positions if the confidence from DeepLabCut was low (<95%). We next used the vertical distance between the upper and lower eyelids to detect blinking, removing pupil position data 100 ms before and 400 ms after each detected blink to eliminate blink-artefacts. We then removed periods of pupil position data when the pupil area was changing rapidly, as asymmetrical dilation or constriction of the pupil could be erroneously interpreted as changes in position. Finally, we filled small gaps in the pupil position stream using linear interpolation to facilitate saccade detection.

To convert the filtered pupil position from pixels to degrees, we set the pupil position for each trial relative to the median position prior to motion onset. Pupil displacement was then converted to millimetres based on objects of known length in the video frame, digitized for each recording session using ImageJ 1.53k [45]. We removed data for trials in which the corneal reflection moved more than 1 mm, as this indicated that the bird rolled its head during the trial (6.7% of total trials). Finally, we converted displacement to degrees based on the assumption that the avian eye rotates around the midpoint between the pupil and the back of the eye [46]. We determined this value (2.181 ± 0.102 mm; mean ± s.d.) by measuring the half distance between the outer edge of the scleral ring and the medial margin of the eye for five eyes from four specimens available from previous laboratory projects. The eye-in-head position was then calculated as $\theta = \tan^{-1}$ (relative position mm/2.181 mm). Importantly, this assumption does not impact the main conclusions of this work and resulted in a similar range of movement to that determined using alternative methods [47].

We next automatically removed saccades using peak detection, analysing the median-filtered velocity of the pupil for spikes above a speed threshold. This speed threshold was manually adjusted (between 5 deg s^{-1} and 15 deg s^{-1}) for each session based on visual inspection of pupil position across trials.

Inspection of the parallel streams of data from each eye indicated that blinks and saccades often occurred simultaneously in both eyes, as in other birds [48,49]. For this reason, we considered a blink or saccade in either eye to constitute a break in OKR and computed the velocities of the eyes between each of these breaks. This allowed us to compare, for the same set of time windows, the motion occurring simultaneously in each eye. To compute OKR velocities, we fit each segment between breaks with a linear regression and extracted the slope (deg s^{-1}), fitted values (deg) and quality of the fit (root mean squared error; RMSE). The magnitudes (deg) of rapid eye movements (blinks and saccades) were determined using these fitted values as the offset between the last and first elements in each adjacent segment.

(f) Statistical analysis

We performed plotting and hypothesis testing in R v. 4.4.0 [50]. For comparisons of OKR between conditions, we removed segments with poor fit quality (RMSE > 0.35) or with many (>10%) missing data points for either eye (together 12.7% of total fits). Significance was assessed by computing bootstrapped means and 95% CIs (1000 iterations) using the R package *boot* [51]. Unless otherwise specified, bootstrapped values were computed by pooling fitted values from both eyes and bootstrapping across trials and individuals.

3. Results

(a) Oculomotor behaviour

We measured the OKR in restrained hummingbirds (figure 1*a*) by presenting sinewave gratings of five spatial frequencies drifting at a range of stimulus speeds (table 1). Hummingbirds responded reliably to visual stimuli with compensatory eye

movements for most stimulus conditions. Shifts in eye-in-head position, measured using video-oculography, were small (figure 1*b*; electronic supplementary material, video 1) but highly repeatable across individuals and trials. Motion onset triggered an almost immediate OKR (typically <250 ms), primarily in the stimulated eye (figure 1*c*). During prolonged stimulus motion, OKR was often interspersed with rapid eye movements that reset the position of the eye, i.e. quick phases, together creating the sawtooth pattern of eye movement known as OKN.

Observations from numerous trials suggested that rapid eye movements frequently occurred during blinking (figure 1*c*). To test whether rapid eye movements were coordinated with blinks, we performed a permutation test. Specifically, we compared the standard deviation of eye position changes during blinks with a distribution of null deviations. Each null value was generated by sampling eye position changes across an equal number of randomly selected time windows, each matched in duration to a blink interval (figure 1*d*). No permutations resulted in a standard deviation greater than that of the actual data ($p < 0.001$), indicating significant synchronization between blinks and rapid eye movements. Blinking (figure 1*e*), detected via the position of the eyelids, and saccades (figure 1*f*), detected via the eye velocity, were also significantly synchronized between the two eyes (non-overlapping 95% CI_{boot} with baseline). As both oculomotor behaviours interrupted slow tracking, we defined the strength of OKR as the velocity of the eye between every blink or saccade (figure 1*g*). The magnitude and direction of rapid eye movements were computed using the offset between adjacent segments of eye position data.

Across conditions, rapid eye movements ranged from maximum values of 8.9 ± 3.3 deg temporal to 8.5 ± 3.4 deg nasal across birds (mean ± s.d.), while the magnitude of OKR ranged from 3.5 ± 0.4 deg temporal to 4.4 ± 1.4 deg nasal.

(b) Monocular optokinetic response

Hummingbirds responded consistently to monocular stimulation across stimulus speeds for sinewave gratings of 0.0625 cyc deg^{-1}, 0.25 cyc deg^{-1} and 1 cyc deg^{-1} (figure 2*a*). The response was greatest to gratings of 1 cyc deg^{-1}, with the stimulated eye consistently reaching speeds during OKR of 2 deg s^{-1} for TN motion at stimulus speeds of 4 deg s^{-1} and 16 deg s^{-1}. OKR to gratings of 0.015625 cyc deg^{-1} was weak relative to higher spatial frequencies, except for 4 cyc deg^{-1}, for which there was no detectable response (figure 2*a*). Thus, we focused subsequent analysis on the three intermediate spatial frequencies. We also subtracted the median response to gratings of 4 cyc deg^{-1} from all other data, grouped by bird, to correct for any individual-specific offsets from zero. To compare the strength of OKR across stimulus directions and stimulus speeds, we converted values of OKR velocity to OKR speed, defined as the magnitude of eye velocity relative to the stimulus direction, for both the stimulated (figure 2*b*) and unstimulated eye (figure 2*c*).

The strength of monocular OKR was asymmetrical, as the speed of the eye during OKR varied with the direction of stimulus. However, the direction that generated the strongest OKR also varied with spatial frequency and stimulus speed. For the three spatial frequencies that generated a consistent response, OKR in the stimulated eye was stronger for NT than TN motion at the lowest stimulus speed but stronger for TN than NT motion at higher stimulus speeds (figure 2*b*; non-overlapping 95% CI_{boot}). This reversal in asymmetry was made more evident by calculating OKR gain (figure 2*d*). For gratings of 1 cyc deg^{-1} and 0.25 cyc deg^{-1}, NT motion at 0.25 deg s^{-1} evoked near-perfect visual compensation (gain ≈ 1), whereas compensation for TN motion was significantly weaker (non-overlapping 95% CI_{boot}). NT motion also evoked better compensation for gratings of 0.0625 cyc deg^{-1} drifting at 1 deg s^{-1} than did TN motion at the same stimulus speed. At higher stimulus speeds, the gain to TN motion surpassed that to NT motion across spatial frequencies, with the reversal of asymmetry occurring between stimulus speeds of 1 deg s^{-1} and 4 deg s^{-1}.

Response values for the unstimulated eye were close to zero for NT stimulation but slightly negative for TN stimulation, indicating weak yoking between the eyes during OKR (figure 2*c*).

(c) Binocular optokinetic response—rotation

OKR tuning across spatial frequencies and stimulus speeds was similar for rotational binocular stimulation (figure 3*a*). Despite simultaneous presentation, clear differences existed between the eye presented with TN motion and the eye presented with NT motion. As with monocular OKR, gratings of 1 cyc deg^{-1} evoked the strongest response, with the eye consistently exceeding speeds of 2 deg s^{-1} when presented TN motion at 4 deg s^{-1} and 16 deg s^{-1}. Across spatial frequencies, NT motion at the lowest stimulus speeds evoked a stronger response than TN motion, but the reverse was true at higher stimulus speeds (non-overlapping 95% CI_{boot}).

The asymmetrical response to binocular rotational stimulation suggested a high level of independence between the eyes, consistent with the weak yoking we measured during monocular stimulation (figure 2*c*). To explore this independence further, we compared the change in position of the left and right eyes for the complete set of matched time bins across all stimulus conditions, separating slow (OKR) and rapid eye movements. In this analysis, conjugate eye movements fall along the negative diagonal, while pure vergence eye movements fall along the positive diagonal (figure 3*c*). Plotting slow eye movements revealed distributions consistent with ocular independence, as most eye movements fell off both conjugate and vergence axes (figure 3*d*). Distributions at each spatial frequency possessed tails projected in positive directions, reflecting stronger OKR to TN motion for most stimulus conditions. The distributions of rapid eye movements were aligned with the conjugate axis, although with off-axis spread of 5 deg or greater (figure 3*d*).

The difference between distributions of OKR and rapid eye movements indicates that not all rapid eye movements that we measured were quick phases. This is expected given that not all stimulus conditions elicited OKR and hummingbirds were free to make gaze changes unrelated to stimulus motion. To further explore the connection between OKR and rapid eye movements,

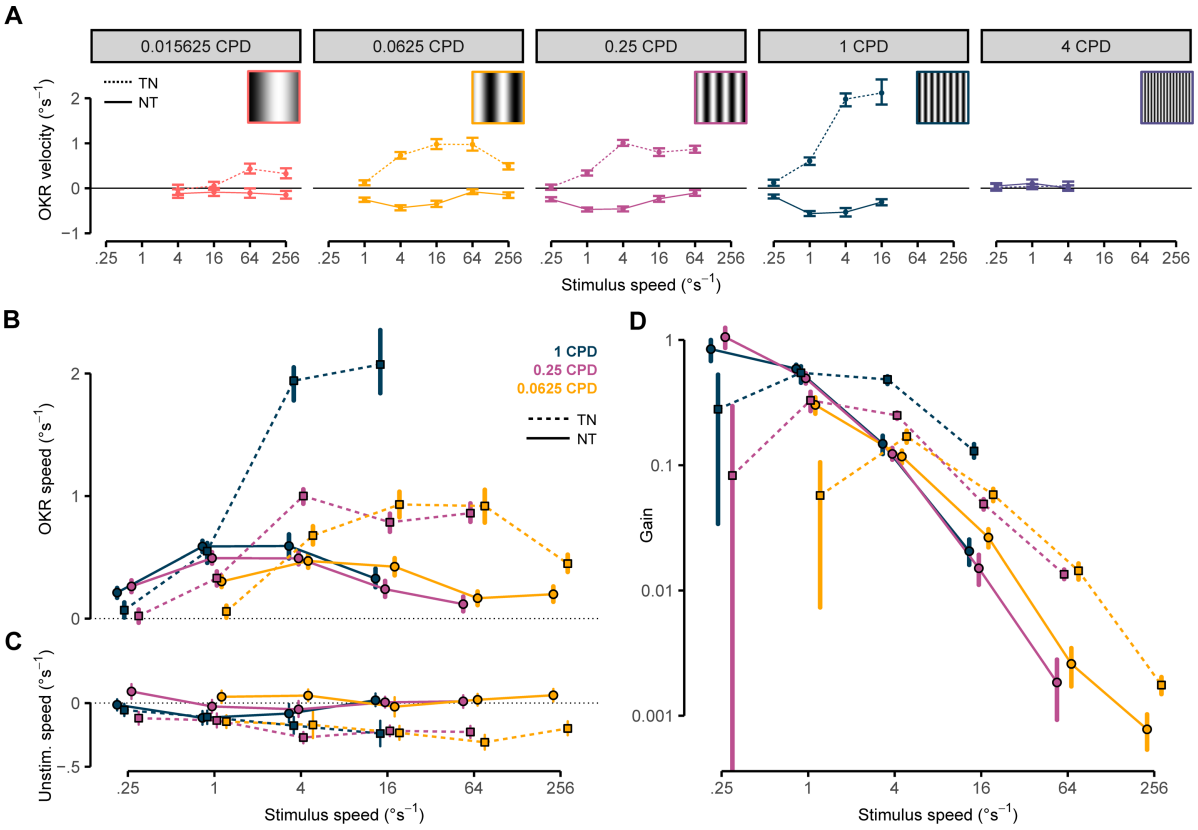

Figure 2. Monocular OKR across spatial frequencies and stimulus speeds. Eye movement data for TN stimulation are shown as dashed lines; data for NT stimulation are shown as solid lines. Stimulus speeds plotted on a logarithmic scale. (A) Mean velocity and 95% CI_{boot} of the stimulated eye during OKR across spatial frequencies and speeds. Positive values indicate nasalward velocities; negative values indicate temporalward velocities. The response to gratings of 0.015625 cyc deg^{-1} was weak and only present at high stimulus speeds. Consistent OKR occurred at the intermediate spatial frequencies of 1 cyc deg^{-1}, 0.25 cyc deg^{-1} and 0.0625 cyc deg^{-1}. Birds did not respond to gratings of 4 cyc deg^{-1}. Inset images of gratings are for illustrative purposes only. (B) Speed of the stimulated eye during OKR across three spatial frequencies for which hummingbirds responded consistently in their stimulated eye (mean and 95% CI_{boot}). Response to NT stimulation was stronger than that to TN stimulation at the slowest tested stimulus speed for each spatial frequency; however, the opposite was true for higher stimulus speeds (non-overlapping 95% CI_{boot}). (C) Speed of the unstimulated eye across three spatial frequencies (mean and 95% CI_{boot}). Yoked responses were present in the unstimulated eye when the stimulated eye viewed TN motion, but these responses were weaker than in the stimulated eye. (D) Gain of OKR (ratio of eye speed to stimulus speed) for the stimulated eye across three spatial frequencies (mean and 95% CI_{boot}). Data presented on a log–log scale for visibility. CPD, cyc deg^{-1}

we compared the magnitude of slow and subsequent rapid eye movements across stimulus conditions (figure 3*e*). A high density of points fell along the negative diagonal during rotational stimulation, indicating that rapid eye movements frequently reset the eye position to the onset position of the previous tracking phase, although spontaneous eye movements were also apparent. During translational stimulation, fewer points fell along this diagonal, indicating greater independence between OKR and rapid eye movements.

(d) Binocular optokinetic response—translation

Hummingbirds responded to translational stimulation with compensatory eye movements for most stimulus conditions (figure 3*b*), although the response was weaker than monocular (figure 2*b*) and rotational OKR (figure 3*a*). Analogous to both monocular OKR and binocular rotational OKR, progressive motion evoked a stronger response than regressive motion at the lowest stimulus speeds, but the opposite was true at higher stimulus speeds, at least for gratings of 1 cyc deg^{-1} and 0.25 cyc deg^{-1}.

The extent of OKR to progressive stimulation was unexpected based on data from other lateral-eyed animals. Importantly, this response could be erroneously observed if hummingbirds made small head movements or if the eyes alternated between compensatory drifts in one eye and no movement in the other. To verify our method of restraint, we digitized 10 features on the face and bill of two hummingbirds [52] and compared simultaneous head and eye displacement in millimetres for four regressive (figure 4*a*) and four progressive trials (figure 4*b*). While there were slight shifts in head position, these head movements were insufficient to explain concurrent eye movements (figure 4*c*).

We also verified that compensatory drifts occurred simultaneously in both eyes and were consistent across individuals by computing the proportion of convergent (both eyes drifting TN) or divergent (both eyes drifting NT) OKR during regressive and progressive stimulation, respectively (figure 4*d*). We used the data from 4 cyc deg^{-1} to generate null distributions, as OKR was absent at this spatial frequency. At most stimulus speeds, the fractions of convergent and divergent eye movements were significantly greater than the null expectation (non-overlapping 95% CI_{boot}). Only at a spatial frequency of 1 cyc deg^{-1} and stimulus speed of 1 deg s^{-1}, however, did all birds consistently exhibit divergent OKR to progressive motion. For regressive motion, all birds consistently exhibited convergent OKR for 1 cyc deg^{-1} at both 1 deg s^{-1} and 4 deg s^{-1}.

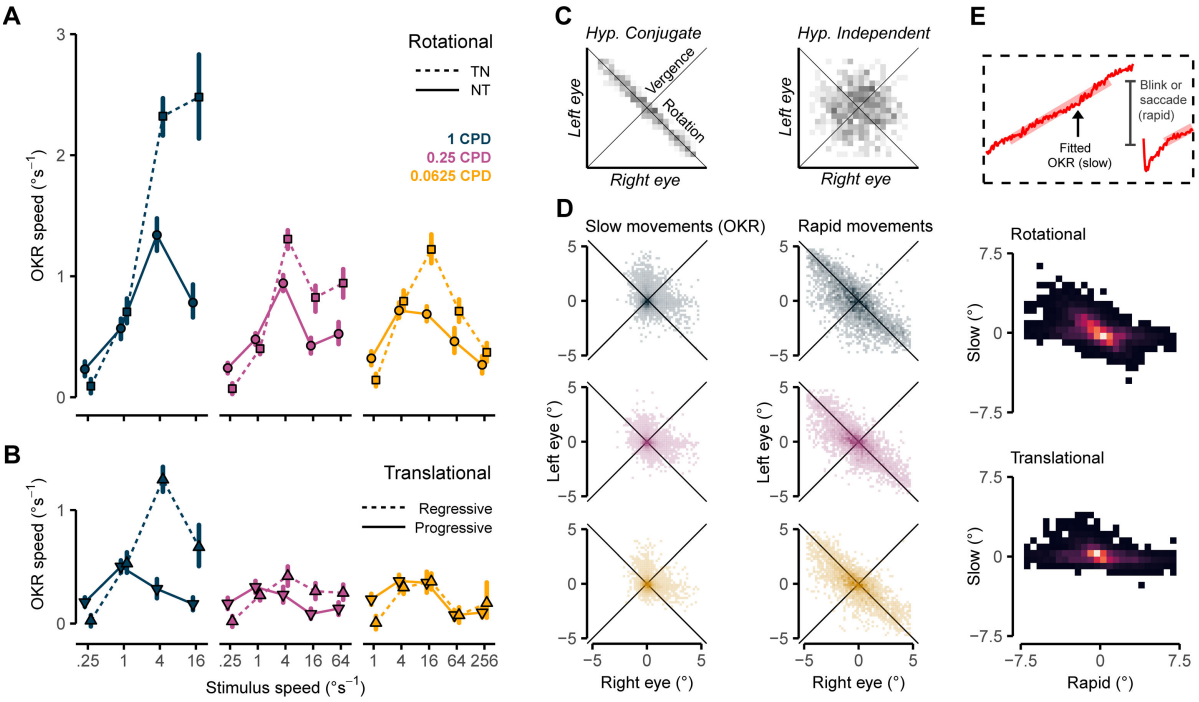

Figure 3. Binocular OKR across spatial frequencies and stimulus speeds. (A) OKR speed for rotational stimulation (mean and 95% CI_{boot}). Data for the eye viewing TN stimuli are shown as dashed lines; data for the eye viewing NT stimuli are shown as solid lines. Stimulus speeds plotted on a logarithmic scale. Response in the eye viewing NT motion was stronger than in the eye viewing TN motion at the slowest tested speeds; however, the opposite was true for higher stimulation speeds (non-overlapping 95% CI_{boot}). (B) OKR speed for translational stimulation (mean and 95% CI_{boot}). Both eyes viewed either TN motion (regressive) or NT motion (progressive). Stimulus speeds plotted on a logarithmic scale. Response to progressive stimulation was stronger than to regressive stimulation at the slowest tested speed for each spatial frequency. For spatial frequencies of 1 cyc deg^{-1} and 0.25 cyc deg^{-1}, the opposite is true for higher stimulation speeds (non-overlapping 95% CI_{boot}). (C) Hypothetical relationship between movements co-occurring in each eye. Position changes for the left eye are plotted on the *y*-axis; position changes for the right eye plotted on the *x*-axis. Distribution indicative of strictly conjugate/yoked movements (left) versus independence (right). Conjugate movements fall along the negative diagonal ('Rotation' axis), while vergence movements fall along the positive diagonal ('Vergence' axis). (D) Movements co-occurring in each eye (see (C) for details). Left column—Slow eye movements co-occurring in each eye. The motion of one eye occurred largely independent of the motion in the other eye, frequently departing from the conjugate and vergence axes. Right column—Rapid eye movements co-occurring in each eye. Distributions aligned with the conjugate axis but with substantial spread. The discordance between the distributions of slow (left) and rapid (right) eye movements indicates that not all rapid eye movements were resets (i.e. quick phases) but also included spontaneous and approximately conjugate movements. (E) Slow versus subsequent rapid eye movements during rotational and translational binocular stimulation. The signature of nystagmus was visible for rotational stimulation, indicated by the high density of points along the negative diagonal—i.e. rapid eye movements frequently reset the eye position from the previous OKR phase, although spontaneous saccades are also apparent. For translatory stimulation, fewer points fell along this diagonal, indicating greater independence between slow and rapid phases. CPD, cyc deg^{-1}.

To further investigate this behaviour, we repeated binocular experiments with gratings of 1 cyc deg^{-1} and an expanded range of stimulus speeds (figure 4*e*). During no-motion trials, eye velocity combinations clustered around the origin. For stimulus at 1 deg s^{-1} and 2 deg s^{-1}, four clusters appeared, indicating that hummingbirds were capable of convergent, divergent, clockwise and counterclockwise OKR at these stimulus speeds. Divergent OKR was absent at higher stimulus speeds (4, 8 and 16 deg s^{-1}), with most points falling above the conjugate axis, indicating some amount of convergence even during rotational stimulation.

4. Discussion

We measured oculomotor behaviour in Anna's hummingbirds, demonstrating that hummingbirds make compensatory eye movements in response to visual motion (figure 1*c*). These eye movements are small but similar in magnitude to those in other non-passerines [53,54] and consistent with measurements of ocular range-of-motion in hummingbirds [47]. Rapid movements occurred simultaneously in both eyes and frequently coincided with blinking (figure 1*d–f*), suggesting that blinking functions as a mechanism for saccadic suppression [55] and that coordination between gaze shifts and blinking may be a general phenomenon across birds [56]. The distribution of rapid eye movements aligned with the conjugate axis, suggesting some degree of yoking, but with substantial spread. Slow tracking eye movements in one eye occurred largely independent of those in the other (figure 3*d*). Under monocular stimulation, yoked eye movements were sometimes visible in the non-stimulated eye, but these rotations were almost always minor relative to those in the stimulated eye (figure 2*c*). Weak coupling between the eyes is similar to that reported in other avian species [48,54], as well as in chameleons [57] and turtles [58]. Consistent with the conclusion that eye movements in hummingbirds are largely independent of one another, all tested animals exhibited compensatory eye movements in response to translational visual motion (figure 4*d*).

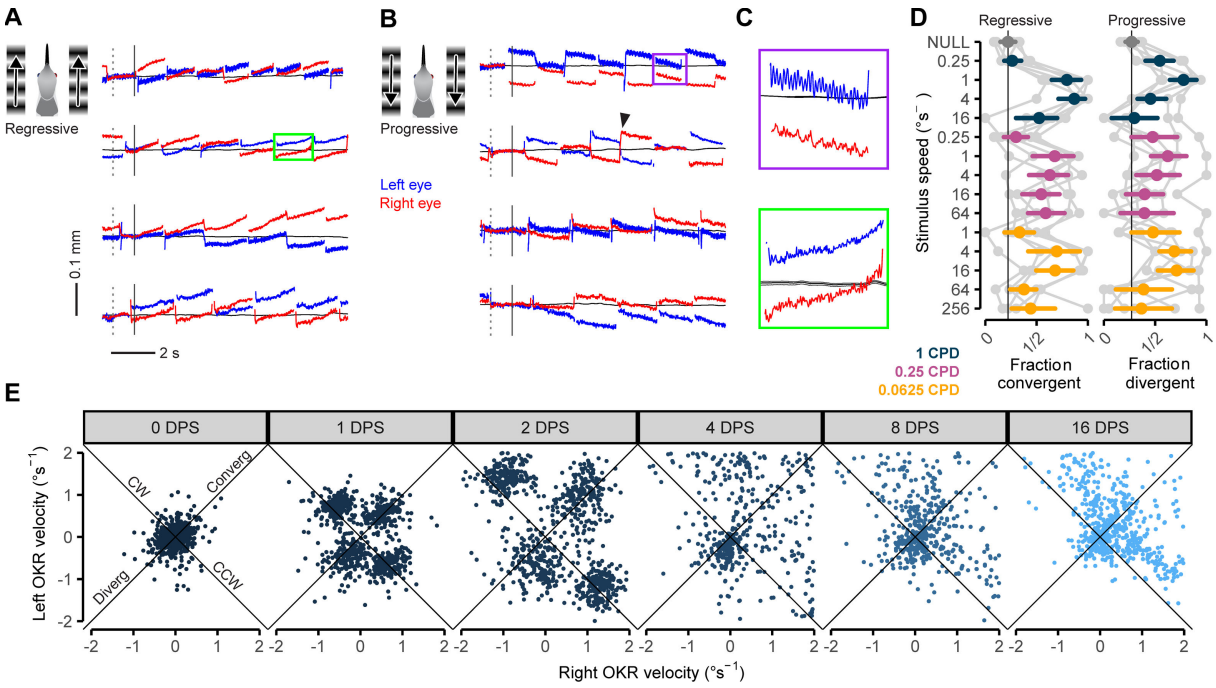

Figure 4. Hummingbirds exhibit convergent and divergent OKR. (A) Position (in millimetres) of the left (blue) and right (red) eyes relative to position of the head (black) during regressive visual motion. Dashed vertical lines indicate grating onset; solid vertical lines indicate stimulus motion onset. Representative data from two individuals are shown (first and second examples are from one individual; third and fourth from the second individual) for two speed-by-spatial frequency combinations (0.25 cyc deg^{-1} and 4 deg s^{-1}, 1 cyc deg^{-1} and 1 deg s^{-1}). Positive is defined as nasalward for both eyes. Birds exhibited convergent OKR, as both eyes moved nasalward in response to regressive visual motion. This effect was not driven by head movements, as the position of the head was relatively stable across trials. The green box corresponds to the zoomed region in the lower half of (C). (B) Same as in (A) but for progressive visual motion. The bird exhibited divergent OKR, as both eyes moved temporalward in response to progressive visual motion. The purple box corresponds to the zoomed region in the upper half of (C). The black arrow indicates a pair of rapid eye movements that failed to reset the position of the eyes from the previous OKR. Axis labels and units are the same as in (A). (C) Regions of divergent (top) and convergent OKR (bottom), selected from examples on the left, magnified to illustrate that changes in head position (black center line: mean position from 10 landmarks, grey shaded region with black outline: 95% CI$_{boot}$) were insufficient to explain translational OKR. (D) Fraction of convergent (both eyes moving nasalward) and divergent (both eyes moving temporalward) eye movements in response to regressive and progressive visual motion, respectively. Null distributions were generated using data from the same stimulus direction at a spatial frequency of 4 cyc deg^{-1}. Fractions were computed both within each individual (light grey points and lines) and across individuals (coloured points and error bars; mean and 95% CI$_{boot}$). Data from the same individual for different stimulus conditions are connected by light grey lines spanning stimulus conditions. Fractions computed across individuals were significantly different from the null for multiple conditions (non-overlapping 95% CI$_{boot}$), indicating that birds exhibited OKR to translational stimulus motion with both eyes, simultaneously. (E) Data from an additional experiment (same 6 birds; 3 weeks after the previous experiments) at an expanded range of speeds (spatial frequency: 1 cyc deg^{-1}) to confirm convergent and divergent OKR. Only rotational and translational stimuli were presented. OKR velocities of the right eye are plotted on the *x*-axis; OKR velocities of the left eye on the *y*-axis. For non-moving stimuli (0 deg s^{-1}), eye velocities clustered around the origin, as expected. For stimuli moving at 1 deg s^{-1} and 2 deg s^{-1}, four clusters appeared, indicating that hummingbirds made convergent, divergent, clockwise and counterclockwise OKR at these speeds. Divergent OKR was absent at higher velocities. Most velocity combinations fell above the conjugate axis, indicating some degree of convergence even during rotational stimulation. CPD, cyc deg^{-1}; DPS, deg s^{-1}; Diverg, divergent movements; Converg, convergent movements; CW, clockwise movements; CCW, counterclockwise movements.

(a) Optokinetic response asymmetry

For many species with lateral eyes, like hummingbirds, the strength of OKR is greater for TN motion than for NT motion (reviewed by [13]). This asymmetry is hypothesized to serve an adaptive function by suppressing compensatory eye movements during forward locomotion (which generates primarily NT visual motion), preserving optic flow for self-motion perception [15–19]. We hypothesized that OKR in hummingbirds would be symmetrical, given that hummingbirds locomote in all directions and rely on optic flow to control these behaviours [9,10]. In addition, LM—the region of the brain responsible for TN OKR in other birds—lacks an overall direction bias in hummingbirds.

Instead, OKR in hummingbirds was asymmetrical, but the direction of asymmetry depended on stimulus speed. At the lowest speeds, hummingbirds responded more strongly to NT motion, whereas at higher speeds responses were stronger for TN motion. For some species with asymmetrical monocular OKR, binocular rotational stimulation can enforce symmetrical OKR [16]. In hummingbirds, however, the pattern of asymmetry was robust across both monocular and binocular stimulation. OKR to high stimulus speeds and with low spatial frequencies was relatively weak, inconsistent with the proportion of hummingbird LM neurons tuned to these and similar stimulus conditions [7,33].

The mismatch between the spatiotemporal and direction tuning of the hummingbird LM and their OKR was unexpected. One potential explanation is that the hummingbird LM contains two separate populations of neurons, both responsive to image slip, but with one population mediating OKR and the other mediating OMR (or flight, more generally). When scaled for brain size, the LM of hummingbirds is 2–5 times larger than in non-hovering birds [8]. Thus, electrophysiology studies may have sampled more 'OMR neurons' than 'OKR neurons'. Hovering OMR in hummingbirds is approximately symmetrical [5,10],

consistent with the lack of overall direction bias across LM neurons. Importantly, electrophysiology studies do report some neurons responsive to slow speeds and high spatial frequencies [7,33], documenting the neural substrate necessary to drive the OKR tuning that we observed.

(b) Disjunctive optokinetic response

Translational stimulation evoked convergent and divergent OKR in hummingbirds. In other words, hummingbirds make simultaneous and disjunctive compensatory eye movements in response to regressive and progressive visual motion, respectively. This response was unexpected given previous studies in vertebrates. Goldfish and butterflyfish, which have laterally placed eyes and yoked eye movements, were found to exhibit convergence to regressive stimuli but were insensitive to progressive stimuli [17,26]. Sandlance and pipefish, on the other hand, exhibited both convergent and divergent OKR [26]. The latter two fish species were specifically chosen for study owing to their 'chameleon-like independent eye movements' [26]. Both pipefish and sandlance exhibited temporally uncoupled eye movements, whereas we found that eye movements in hummingbirds were temporally coupled between the two eyes, as is the case in chameleons [57].

Collewijn and Noorduin [16] showed that translational stimuli resulted in weak vergence in rabbits; however, the movements of both eyes were often asymmetrical, with compensation occurring in only one eye, and the eyes often remained stationary after reaching a maximal position [16]. By contrast, translational OKR in hummingbirds was always interrupted by rapid eye movements, and compensation in both eyes was frequently symmetrical. Studies of translational OKR are rare, potentially owing to limited response by early model organisms [16,17] and the widely held assumption that OKR during forward locomotion would be maladaptive [15–19]. Surprisingly, our results align closely with recent work on another flying animal, *Drosophila*, in which the retina shifts to compensate for rotational and translational visual motion [59].

Avian eye movements are typically exaggerated during head-restraint [18]. Thus, it is unclear whether hummingbirds would exhibit convergent or divergent OKR during flight. We were unable to study oculomotor behaviour in free-moving animals because bright pupil tracking requires near-perfect alignment between the optical axes of the eye and camera, and the hummingbird pupil is undetectable under ambient light. Larval zebrafish exhibit divergent OKR [27], but only when restrained [60]. Free-swimming zebrafish instead compensate for translational stimuli through an optomotor response. However, an important distinction between our study and those on zebrafish is that most fish species cannot blink. We show that hummingbirds synchronize rapid gaze shifts with blinks, similar to other birds [56]. Primates exhibit stronger compensatory responses to visual motion immediately after making a rapid eye movement [61,62]—a phenomenon referred to as post-saccadic enhancement—which functions to quickly re-establish stable vision after it has been suppressed [63]. Thus, frequent blinking in hummingbirds may facilitate disjunctive OKR during free movement by enhancing subsequent compensatory responses.

Hummingbird slow and rapid eye movements appear largely uncorrelated with each other during translational stimulation, unlike for monocular or rotational stimulation (figure 3*e*). Thus, we refer to this behaviour as disjunctive OKR rather than disjunctive OKN. OKN is a rhythmic pattern of eye movement in which the quick phase resets the position of the eye from the previous slow phase. Instead, for translational stimuli, rapid eye movements in hummingbirds may move either against or with stimulus motion (figure 4*b*). This pattern of eye movement is reminiscent of that in humans and non-human primates when viewing optic flow fields. Under these conditions, primates make exploratory saccades followed by smooth tracking of whatever stimulus motion occurs at the saccadic endpoint [64,65]. This is also true for humans during free movement [66], together suggesting a potential role for disjunctive OKR during flight in hummingbirds. This behaviour would potentially complicate the perception of self-motion from optic flow, but could facilitate detection of object motion (e.g. conspecifics, predators) because moving objects are easier to detect against a stable background [67].

Ethics. All procedures were reviewed and approved by the Animal Care Committee of the University of British Columbia (protocol A23−0146). Animals were collected under scientific collecting permit SC-BC−2023–0001 and released after the experiments described herein.

Data accessibility. High-quality MP4 versions of all eye-tracking videos, along with all data and code used for analysis, are available on Dryad [68]. AVI versions of eye-tracking videos are available upon request owing to the size of these uncompressed files. Supplementary material is available online.

Declaration of AI use. We used DeepLabCut—a machine learning approach—to automate a portion of kinematic tracking (see §2). We used ChatGPT as a 'search engine' to suggest suitable code functions for analysis.

Authors' contributions. A.B.L.: conceptualization, data curation, formal analysis, investigation, methodology, software, validation, visualization, writing—original draft, writing—review and editing; P.K.: conceptualization, investigation, methodology, validation, writing—review and editing; M.S.: conceptualization, funding acquisition, project administration, supervision, writing—review and editing; D.R.W.: conceptualization, methodology, supervision, writing—review and editing; D.L.A.: conceptualization, funding acquisition, project administration, resources, validation, writing—review and editing.

All authors gave final approval for publication and agreed to be held accountable for the work performed therein.

Conflict of interest declaration. We declare we have no competing interests.

Funding. This work was supported by an NSERC Discovery Grant (RGPIN−2021–02977) awarded to D.L.A. and a Djavad Mowafaghian Centre for Brain Health Kickstart Grant awarded to D.L.A. and M.S. Support for A.B.L. was provided by postdoctoral fellowships from the Michael Smith Health Research BC / Parkinson Society British Columbia (RT−2023–3226) and the National Science Foundation (2109873).

Acknowledgements. We thank Sylvia Heredia for the creation of artwork and animation. We thank Robert Shadwick for laboratory space used for these experiments.

References

1. Portugues R, Engert F. 2009 The neural basis of visual behaviors in the larval zebrafish. *Curr. Opin. Neurobiol*. **19**, 644–647. (doi:10.1016/j.conb.2009.10.007)
2. Wibble T, Pansell T, Grillner S, Pérez-Fernández J. 2022 Conserved subcortical processing in visuo-vestibular gaze control. *Nat. Commun*. **13**, 4699. (doi:10.1038/s41467-022-32379-w)
3. Angelaki DE, Hess BJM. 2005 Self-motion-induced eye movements: effects on visual acuity and navigation. *Nat. Rev. Neurosci*. **6**, 966–976. (doi:10.1038/nrn1804)
4. Nakayama K. 1981 Differential motion hyperacuity under conditions of common image motion. *Vision Res*. **21**, 1475–1482. (doi:10.1016/0042-6989(81)90218-2)
5. Baliga VB, Dakin R, Wylie DR, Altshuler DL. 2024 Hummingbirds use distinct control strategies for forward and hovering flight. *Proc. R. Soc. B* **291**, 20232155. (doi:10.1098/rspb.2023.2155)
6. Dakin R, Fellows TK, Altshuler DL. 2016 Visual guidance of forward flight in hummingbirds reveals control based on image features instead of pattern velocity. *Proc. Natl Acad. Sci. USA* **113**, 8849–8854. (doi:10.1073/pnas.1603221113)
7. Gaede AH, Goller B, Lam JPM, Wylie DR, Altshuler DL. 2017 Neurons responsive to global visual motion have unique tuning properties in hummingbirds. *Curr. Biol*. **27**, 279–285. (doi:10.1016/j.cub.2016.11.041)
8. Iwaniuk AN, Wylie DRW. 2007 Neural specialization for hovering in hummingbirds: hypertrophy of the pretectal nucleus lentiformis mesencephali. *J. Comp. Neurol*. **500**, 211–221. (doi:10.1002/cne.21098)
9. Goller B, Segre PS, Middleton KM, Dickinson MH, Altshuler DL. 2017 Visual sensory signals dominate tactile cues during docked feeding in hummingbirds. *Front. Neurosci*. **11**, 622. (doi:10.3389/fnins.2017.00622)
10. Goller B, Altshuler DL. 2014 Hummingbirds control hovering flight by stabilizing visual motion. *Proc. Natl Acad. Sci. USA* **111**, 18375–18380. (doi:10.1073/pnas.1415975111)
11. Ros IG, Biewener AA. 2016 Optic flow stabilizes flight in ruby-throated hummingbirds. *J. Exp. Biol*. **219**, 2443–2448. (doi:10.1242/jeb.128488)
12. Goller B, Fellows TK, Dakin R, Tyrrell L, Fernández-Juricic E, Altshuler DL. 2019 Spatial and temporal resolution of the visual system of the Anna's hummingbird (*Calypte anna*) relative to other birds. *Physiol. Biochem. Zool*. **92**, 481–495. (doi:10.1086/705124)
13. Masseck OA, Hoffmann KP. 2009 Comparative neurobiology of the optokinetic reflex. *Ann. N. Y. Acad. Sci*. **1164**, 430–439. (doi:10.1111/j.1749-6632.2009.03854.x)
14. Tauber ES, Atkin A. 1967 Disconjugate eye movement patterns during optokinetic stimulation of the African chameleon, *Chameleo melleri*. *Nature* **214**, 1008–1010. (doi:10.1038/2141008b0)
15. Brodsky MC. 2021 Monocular nasotemporal optokinetic asymmetry—unraveling the mystery. In *The evolutionary basis of strabismus and nystagmus in children* (ed. M Brodsky), pp. 225–229. Cham, Switzerland: Springer International Publishing. (doi:10.1007/978-3-030-62720-1_19)
16. Collewijn H, Noorduin H. 1972 Conjugate and disjunctive optokinetic eye movements in the rabbit, evoked by rotatory and translatory motion. *Pflugers Arch*. **335**, 173–185. (doi:10.1007/BF00592155)
17. Easter SS. 1972 Pursuit eye movements in goldfish (*Carassius auratus*). *Vision Res*. **12**, 673–688. (doi:10.1016/0042-6989(72)90161-7)
18. Land MF. 2015 Eye movements of vertebrates and their relation to eye form and function. *J. Comp. Physiol. A* **201**, 195–214. (doi:10.1007/s00359-014-0964-5)
19. Wallman J. 1993 Subcortical optokinetic mechanisms. In *Visual motion and its role in the stabilization of gaze* (eds F Miles, J Wallman), pp. 321–338. Amsterdam, The Netherlands: Elsevier.
20. Krapp HG. 2013 Optic flow processing. In *Encyclopedia of computational neuroscience* (eds D Jaeger, R Jung), pp. 1–22. New York, NY: Springer. (doi:10.1007/978-1-4614-7320-6_332-1)
21. Nakayama K. 1985 Biological image motion processing: a review. *Vision Res*. **25**, 625–660. (doi:10.1016/0042-6989(85)90171-3)
22. Friedman MB. 1975 Visual control of head movements during avian locomotion. *Nature* **255**, 67–69. (doi:10.1038/255067a0)
23. Frost BJ. 1978 The optokinetic basis of head-bobbing in the pigeon. *J. Exp. Biol*. **74**, 187–195. (doi:10.1242/jeb.74.1.187)
24. Kano F, Walker J, Sasaki T, Biro D. 2018 Head-mounted sensors reveal visual attention of free-flying homing pigeons. *J. Exp. Biol*. **221**, jeb183475. (doi:10.1242/jeb.183475)
25. Taylor LA, Taylor GK, Lambert B, Walker JA, Biro D, Portugal SJ. 2019 Birds invest wingbeats to keep a steady head and reap the ultimate benefits of flying together. *PLoS Biol*. **17**, e3000299. (doi:10.1371/journal.pbio.3000299)
26. Fritsches KA, Marshall NJ. 2002 Independent and conjugate eye movements during optokinesis in teleost fish. *J. Exp. Biol*. **205**, 1241–1252. (doi:10.1242/jeb.205.9.1241)
27. Feierstein CE, de Goeij MHM, Ostrovsky AD, Laborde A, Portugues R, Orger MB, Machens CK. 2023 Dimensionality reduction reveals separate translation and rotation populations in the zebrafish hindbrain. *Curr. Biol*. **33**, 3911–3925.(doi:10.1016/j.cub.2023.08.037)
28. Gutiérrez-Ibáñez C, Wylie DR, Altshuler DL. 2023 From the eye to the wing: neural circuits for transforming optic flow into motor output in avian flight. *J. Comp. Physiol. A* **209**, 839–854. (doi:10.1007/s00359-023-01663-5)
29. Gioanni H, Villalobos J, Rey J, Dalbera A. 1983 Optokinetic nystagmus in the pigeon (*Columba livia*). III. Role of the nucleus ectomamillaris (nEM): Interactions in the accessory optic system (AOS). *Exp. Brain Res.* **50**, 248–258. (doi:10.1007/BF00239189)
30. Gioanni H, Rey J, Villalobos J, Richard D, Dalbera A. 1983 Optokinetic nystagmus in the pigeon (*Columba livia*). II. Role of the pretectal nucleus of the accessory optic system (AOS). *Exp. Brain Res.* **50**, 237–247. (doi:10.1007/BF00239188)
31. Gaede AH, Baliga VB, Smyth G, Gutiérrez-Ibáñez C, Altshuler DL, Wylie DR. 2022 Response properties of optic flow neurons in the accessory optic system of hummingbirds versus zebra finches and pigeons. *J. Neurophysiol*. **127**, 130–144. (doi:10.1152/jn.00437.2021)
32. Wylie DR, Frost BJ. 1990 The visual response properties of neurons in the nucleus of the basal optic root of the pigeon: a quantitative analysis. *Exp. Brain Res*. **82**, 327–336. (doi:10.1007/BF00231252)
33. Smyth G, Baliga VB, Gaede AH, Wylie DR, Altshuler DL. 2022 Specializations in optic flow encoding in the pretectum of hummingbirds and zebra finches. *Curr. Biol*. **32**, 2772–2779. (doi:10.1016/j.cub.2022.04.076)
34. Winterson BJ, Brauth SE. 1985 Direction-selective single units in the nucleus lentiformis mesencephali of the pigeon (*Columba livia*). *Exp. Brain Res*. **60**, 215–226. (doi:10.1007/BF00235916)
35. Wylie DRW, Crowder NA. 2000 Spatiotemporal properties of fast and slow neurons in the pretectal nucleus lentiformis mesencephali in pigeons. *J. Neurophysiol*. **84**, 2529–2540. (doi:10.1152/jn.2000.84.5.2529)
36. Eckmeier D, Bischof HJ. 2008 The optokinetic response in wild type and white zebra finches. *J. Comp. Physiol. A Neuroethol. Sens. Neural. Behav. Physiol*. **194**, 871–878. (doi:10.1007/s00359-008-0358-7)
37. Gioanni H, Rey J, Villalobos J, Bouyer JJ, Gioanni Y. 1981 Optokinetic nystagmus in the pigeon (*Columba livia*). *Exp. Brain Res*. **44**, 362–370. (doi:10.1007/BF00238829)

38. Hansen DW, Ji Q. 2010 In the eye of the beholder: a survey of models for eyes and gaze. *IEEE Trans. Pattern Anal. Mach. Intell*. **32**, 478–500. (doi:10.1109/TPAMI.2009.30)
39. Stoddard MC, Eyster HN, Hogan BG, Morris DH, Soucy ER, Inouye DW. 2020 Wild hummingbirds discriminate nonspectral colors. *Proc. Natl Acad. Sci. USA* **117**, 15112–15122. (doi:10.1073/pnas.1919377117)
40. Peirce J, Gray JR, Simpson S, MacAskill M, Höchenberger R, Sogo H, Kastman E, Lindeløv JK. 2019 PsychoPy2: Experiments in behavior made easy. *Behav. Res. Methods* **51**, 195–203. (doi:10.3758/s13428-018-01193-y)
41. Python Software Foundation.2024 Python Language Reference v. 3.11.8. See https://www.python.org/.
42. Mathis A, Mamidanna P, Cury KM, Abe T, Murthy VN, Mathis MW, Bethge M. 2018 DeepLabCut: markerless pose estimation of user-defined body parts with deep learning. *Nat. Neurosci*. **21**, 1281–1289. (doi:10.1038/s41593-018-0209-y)
43. OpenCV Development Team.2024 OpenCV: Open source computer vision library v. 4.9.0. See https://opencv.org.
44. The Mathworks Inc.2023 MATLAB v. 2023b. Natick, Massachusetts, US: The Mathworks Inc. See https://www.mathworks.com/.
45. Schneider CA, Rasband WS, Eliceiri KW. 2012 NIH Image to ImageJ: 25 years of image analysis. *Nat. Methods* **9**, 671–675. (doi:10.1038/nmeth.2089)
46. Schwarz JS, Sridharan D, Knudsen EI. 2013 Magnetic tracking of eye position in freely behaving chickens. *Front. Syst. Neurosci*. **7**, 91. (doi:10.3389/fnsys.2013.00091)
47. Tyrrell LP, Goller B, Moore BA, Altshuler DL, Fernández-Juricic E. 2018 The orientation of visual space from the perspective of hummingbirds. *Front. Neurosci*. **12**, 16. (doi:10.3389/fnins.2018.00016)
48. Tyrrell LP, Butler SR, Fernández-Juricic E. 2015 Oculomotor strategy of an avian ground forager: tilted and weakly yoked eye saccades. *J. Exp. Biol*. **218**, 2651–2657. (doi:10.1242/jeb.122820)
49. Voss J, Bischof HJ. 2009 Eye movements of laterally eyed birds are not independent. *J. Exp. Biol*. **212**, 1568–1575. (doi:10.1242/jeb.024950)
50. R Core Team.2024 R: a language and environment for statistical computing v. 4.4.0. Vienna, Austria: R Foundation for Statistical Computing. See https://cran.r-project.org/.
51. Canty A, Ripley B, Brazzale AR. 2024 Package 'boot'. Bootstrap Functions. CRAN R Project https://cran.r-project.org/web/packages/boot/boot.pdf
52. Hedrick TL. 2008 Software techniques for two- and three-dimensional kinematic measurements of biological and biomimetic systems. *Bioinspir. Biomim.* **3**, 034001. (doi:10.1088/1748-3182/3/3/034001)
53. Lemeignan M, Sansonetti A, Gioanni H. 1992 Spontaneous saccades under different visual conditions in the pigeon. *NeuroReport* **3**, 17–20. (doi:10.1097/00001756-199201000-00004)
54. Wallman J, Pettigrew JD. 1985 Conjugate and disjunctive saccades in two avian species with contrasting oculomotor strategies. *J. Neurosci.* **5**, 1418–1428. (doi:10.1523/JNEUROSCI.05-06-01418.1985)
55. Binda P, Morrone MC. 2018 Vision during saccadic eye movements. *Annu. Rev. Vis. Sci.* **4**, 193–213. (doi:10.1146/annurev-vision-091517-034317)
56. Yorzinski JL. 2016 Eye blinking in an avian species is associated with gaze shifts. *Sci. Rep.* **6**, 32471. (doi:10.1038/srep32471)
57. Frens MA, van Beuzekom AD, Sándor PS, Henn V. 1998 Binocular coupling in chameleon saccade generation. *Biol. Cybern*. **78**, 57–61. (doi:10.1007/s004220050412)
58. Ariel M. 1990 Independent eye movements in the turtle. *Vis. Neurosci*. **5**, 29–41. (doi:10.1017/s0952523800000055)
59. Fenk LM, Avritzer SC, Weisman JL, Nair A, Randt LD, Mohren TL, Siwanowicz I, Maimon G. 2022 Muscles that move the retina augment compound eye vision in *Drosophila*. *Nature* **612**, 116–122. (doi:10.1038/s41586-022-05317-5)
60. Zhang Y, Huang R, Nörenberg W, Arrenberg AB. 2022 A robust receptive field code for optic flow detection and decomposition during self-motion. *Curr. Biol*. **32**, 2505–2516.(doi:10.1016/j.cub.2022.04.048)
61. Busettini C, Miles FA, Krauzlis RJ. 1996 Short-latency disparity vergence responses and their dependence on a prior saccadic eye movement. *J. Neurophysiol*. **75**, 1392–1410. (doi:10.1152/jn.1996.75.4.1392)
62. Kawano K, Miles FA. 1986 Short-latency ocular following responses of monkey. *J. Neurophysiol.* **56**, 1355–1380. (doi:10.1152/jn.1986.56.5.1355)
63. Miles FA. 1998 The neural processing of 3-D visual information: evidence from eye movements. *Eur. J. Neurosci.* **10**, 811–822. (doi:10.1046/j.1460-9568.1998.00112.x)
64. Chow HM, Knöll J, Madsen M, Spering M. 2021 Look where you go: characterizing eye movements toward optic flow. *J. Vis*. **21**, 19. (doi:10.1167/jov.21.3.19)
65. Lappe M, Hoffmann KP, Lappe M. 2000 Optic flow and eye movements. *In. Int. Rev. Neurobiol.* 29–47. (doi:10.1016/S0074-7742(08)60736-9)
66. Muller KS, Matthis J, Bonnen K, Cormack LK, Huk AC, Hayhoe M. 2023 Retinal motion statistics during natural locomotion. *eLife* **12**, e82410. (doi:10.7554/eLife.82410)
67. Land MF, Nilsson DE. 2012 *Animal eyes*, 2nd ed. New York, NY: Oxford University Press.
68. Lapsansky AB, Kreyenmeier P, Spering M, Wylie DR, Altshuler DL. 2024 Hummingbirds use compensatory eye movements to stabilize both rotational and translational visual motion. Dryad Digital Repository (doi:10.5061/dryad.vt4b8gv2g)